

Particle Swarm Algorithm for Optimizing Hyperparameters and Artificial Neural Network Parameters to Predict Nuclear Binding Energy for Some Odd-Mass Isotopes

Ruya H. Ibrahim⁽¹⁾

Department of Physics, College
of Science, University of Anbar,
Ramadi, Iraq.

Roy21s2010@uoanbar.edu.iq

Akram Mohammed Ali⁽²⁾

Department of Physics, College
of Science, University of
Anbar, Ramadi, Iraq

dr.akram@uoanbar.edu.iq

Abstract:

Artificial neural networks (ANNs) are essential machine learning models widely used in various fields and applications. These models rely on a vector of parameters, which must be computationally estimated. In this study, a fully connected multilayer perceptron ANN, a modern feedforward neural network with two input layers and two hidden layers (each containing 10 neurons), was developed to estimate the ground state binding energy of isotopes with odd mass numbers ranging from 17 to 339, covering 3414 nuclei. The ANN was applied to three models: the integrated nuclear model, the liquid drop model (LDM), and an empirical formula. The predicted ground state binding energies were evaluated using mean square error (MSE), correlation coefficient (R), and accuracy. To optimize the ANN's performance, parameters such as the number of hidden layers and learning rates were refined using the particle swarm optimization (PSO) algorithm. This optimization reduced the ANN error, achieving an MSE of 0.0099706 and a high accuracy of 99.736% for the LDM model. The correlation coefficient R demonstrated a strong association between the target and output values, confirming the accuracy and robustness of the models. The PSO algorithm's optimization further minimized errors and improved the results, validating the differences in binding energy between the three models and the ANN. This approach underscores the effectiveness of ANNs in modeling complex physical phenomena with high precision.

Keywords: Artificial neural network, binding energy, mean square error, particle swarm optimization algorithm Error, PSO algorithm.

Introduction:

Over the last ten years, development in deep learning has produced advancements in several fields, such as computer vision (He *et al.*, 2016; Szegedy *et al.*, 2017), natural language processing (Bahdanau, 2014; Vaswani, 2017) and the recognition of speech (Hannun, 2014; Chan *et al.*, 2016). High-performing neural architectures are very important for the success of deep learning in these fields. The automated process of the design of neural architecture for a given task called “Neural architecture search (NAS)” (Hutter, Kotthoff and Vanschoren, 2019) is already overall the best human- design for architecture in the many tasks [8-10] as ImageNet [11] or diverse and less-studied datasets (Shen, Khodak and Talwalkar, 2022). NAS has a large overlap with hyperparameter optimization (HPO) (Feurer and Hutter, 2019), where the hyperparameters get automated optimization. Sometimes NAS is referred to as a subset of HPO, but the two techniques are often different. By NAS, one can find a new state-of-the-art Artificial Neural Network (ANN) for many tasks without any substantial human supervision.

The ANN has emerged as one of the important techniques for modeling nonlinear complexes. However, in recent years, several optimization techniques have been utilized to optimize the materials. One of them is particle swarm optimization (PSO) (Kennedy and Eberhart, 1995), which is based on cooperative behavior among species. So, in this work, we will use these two techniques to establish a novel prediction-optimization (ANN-PSO) model that predicts the nuclear binding energies for nuclei. This approach provides a flexible, useful, and efficient tool for optimizing the datasets of binding energies.

Explanation and BP neural network-based residual interaction prediction model. We are able to compute the nuclear masses of $A \geq 100$ by using a residual interactions model to combine the experimental values (Jiao, 2020a). In 2022, using the artificial intelligence network, the nuclear binding energy, which is one of the most essential basic nuclear characteristics, was described with an accuracy of 0.2 Mev (Zeng *et al.*, 2024). The exact calculation of the mass of the nucleus is considered one of the most important quantities of basic inputs in nuclear physics, and to improve accuracy in the models, artificial neural networks are used, a training method was proposed for the neural network, and thus the results have been improved by 20% from the original results that were calculated by applying the liquid drop model (Li *et al.*, 2022).

One of the crucial things to understand, explain, and rationalize in nuclear physics is how protons and neutrons can be packed into the small volume of the nucleus despite the presence of the Coulomb repulsive force. Therefore, it is necessary to rely on models that explain the phenomena of nuclear structure. One of these phenomena is the binding energy, which depends on the nuclear mass, which is one of the fundamental properties of the atomic nucleus through which the rest of the properties (mass, decay lifetime, reaction rate) are controlled, in addition to other information about the nuclear structure (pairing, shell effect, deformation, etc.) (Lunney et al., 2003). This energy is defined by the empirical formula $BE = [Zmp + Nm_n - M(Z, N)]C^2$ (in a.m.u.) which will be used in this paper as an empirical formula.

In recent years, many studies have been carried out to calculate binding energy values based on the nuclear mass study (Roca-Maza and Piekarewicz, 2008; Mumpower *et al.*, 2016; Utama, Piekarewicz and Prosper, 2016; Kondev and Naimi, 2017) included in AME2003 (Audi, Wapstra and Thibault, 2003), which is an essential database for many experiments and which was updated in 2012 in AME2012 (Wang *et al.*, 2012) and in 2017 in AME2017 (Audi *et al.*, 2017) after the development of experimental equipment and the acquisition of more accurate data. The RMSD for 2353 in AME2012 decreased from 2.455 MeV to 0.235 MeV for the liquid drop model, while for the rest of the models, it decreased by about 30%

(Jiao, 2020b).

Most of these nuclei were not calculated experimentally as most of them were measured from the directions from the mass surface determined by the pairing energy between proton and neutron. While theoretical modeling is fundamental in extrapolating the binding energy even to unknown regions of the nuclear chart, it is also tricky due to the transitions that occur as a result of nuclear interactions and also in the quantitative calculation of the many-body (Garvey and Kelson, 1966; Duflo and Zuker, 1995; Thoennessen, 2018).

The Bethe-Weizsacker (BW) formula is the first predictive formula (Fu *et al.*, 2011; Jiang *et al.*, 2012). Based on macroscopic considerations of a liquid drop-like nucleus without taking into account microscopic effects. However, results using new models such as Density Functional Theory (DFT) and Relativistic Mean-Field (RMF) gave different values from those observed experimentally, with Mean Squared Error (MSE) values of ~3 MeV for the BW model (Costiris *et al.*, 2009; Akkoyun, Bayram and Turker,

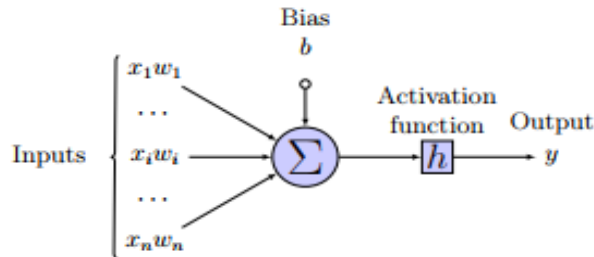
2014), and 0.3 MeV for the WS model (Jiang *et al.*, 2010). The accuracy of these models is not sufficient for the study of nuclear structure, so bells were needed to improve the accuracy of the prediction of the binding energy at any known or unknown mass after the field was narrow.

From these facts, the goal of this research paper will be to use the predictions that the neural network will give about the ground state binding energy using MATLAB 2016b in terms of accuracy, correlation coefficient (R), and mean square error (MSE) after performing the necessary calculations for the empirical formula and two theoretical models, namely the liquid drop model and the Integrated Nuclear Model (INM) that formulated based on the theory of quantum chromodynamics for nuclei with an odd mass number within the nuclear chart. This detailed understanding of the nuclear binding energy of nuclei of known or unknown mass will provide the possibility of obtaining a more accurate map of nuclei with essential applications in nuclear physics and astrophysics. Obtaining the MSE from ANN (which uses two inputs and two hidden layers to create a single input) data will enable us to compare these results with available experimental data. Then, to obtain more accurate results and reduce the error rate to optimize the reduction of the results, a PSO algorithm optimization function will be used that gives better performance for the accuracy of the results. The selected initialization ANN was optimized by the PSO algorithm to predict binding energies, which is called the PSO-ANN model. In this regard, the parameters of the PSO algorithm were set up, including the number of particle swarms (S_w). Consequently, it will be used to optimize the number of hidden layers and learning rate of the ANN and reduce ANN error by comparing the results with the output values, mean square error of the target values, and results calculated by the ANN. The reason we used this method is one of the modern methods used to predict theoretical results that can be compared with practical results and can be used in many applications in the field of physics, especially nuclear physics, where reactions can be studied or any other applications related to nuclear physics.

ANN Construction:

In the past few years, algorithms based on machine learning have appeared, which have been widely used in many studies (Utama and Piekarewicz, 2017, 2018). One of these algorithms is the Artificial Neural Network (ANN), which is a computer model that is based on the architecture and operation of neural networks in the human brain; alternatively, it is a structure composed of connected, adaptive SPUs, occasionally referred to as artificial neurons.

Figure 1 is organized into layers: input, hidden, and output. The weight of each neuronal link determines the signal strength. By adjusting these weights based on data, ANNs are trained to identify patterns and relationships in the data. They are extensively employed in machine learning for a variety of



applications, such as natural language processing and image recognition (Takamoto *et al.*, 2022).

Figure 1. A single model neuron (Bishop, 2006).

Understanding Artificial Neural Networks (ANNs) and how they work requires many essential formulas (Hassoun, 1995; Bishop, 2006). The activation function, which determines the weighted inputs of each artificial neuron, can be linear (ReLU), threshold, sigmoid (σ), step, Gaussian, rectified linear unit function, etc. The formula is used to get the weighted sum of inputs to a neuron.

$$\text{Weighted Sum} = \sum_{i=1}^n (\omega_i \times x_i) + b \quad (1)$$

where ω_i is the weight of the *ith* input, x_i is the *ith* input value, n is the number of inputs, and b is the bias term. The mass data was taken from AME2020 (Wang *et al.*, 2021) and included 3414 nuclei. Two input layers, two hidden layers (10 neurons per layer), and one output layer were selected for the ANN. Training calculation using the TRINLM function is shown in Figure 2.

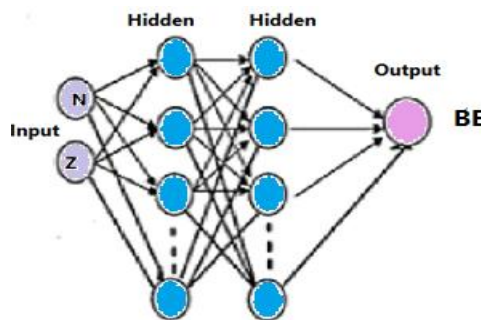


Figure 2. Show two input features (Z, N), hidden layers of ten nodes, and output (B.E) we use in ANN.

A learning rule is used to update the connection weights during training. The backpropagation algorithm is one typical learning guideline. Depending on the job, various metrics are commonly used to calculate the error (or loss) of the network's projections. For regression tasks, the Mean Squared Error (MSE) is frequently utilized. A hyperparameter that controls the weight of the gradient descent is updated by the learning rate. It regulates the rate at which the network converges on a solution.

Particle Swarm Optimization (PSO) Algorithm:

Kennedy and Eberhart initially suggested the technique known as particle swarm optimization (PSO) in 1995 (Kennedy and Eberhart, 1997). In the statistical world, this was regarded as an adaptive computation approach that had numerous benefits. It can be used in nuclear physics due to its robustness, capacity for worldwide exploration, and simplicity of application. Therefore, in order to better understand binding energy, we will use it in relation to each particle's position (z_i) and velocity (v_i) (Phommixay, Doumbia and Lupien St-Pierre, 2020). That given as:

$$z_i(t+1) = z_i(t) + v_i(t+1) \quad (2)$$

$$v_i(t+1) = \omega v_i + c_1 \times \alpha_1 \times [pbest(t) - z_i(t)] + c_2 \times \alpha_2 [gbest(t) - z_i(t)] \quad (3)$$

on the right side of Eq.3, the first term represents the effect of the motion of particular particles, where W is the weight of inertia; the second term represents individual perception, which is based on the previous behavior of the particle (the particle compares its position with the previous best ($Pbest_t$)); the third term represents the social aspect of intelligence, based on a comparison of the position of the particle and the best result obtained by the best swarm ($gbest_t$). Eq.2 describes how positions are updated. Both (α_1 and α_2) are uniformly distributed random numbers in the range [0,1] in this work; (c_1 and c_2) are acceleration constants, z constriction factor, in our work $=0.729$. The weight of inertia has two values $W_{max}=0.9$, $W_{min}=0.4$. A Solution for our specific problem will be represented by the multi-dimensional position of a particle and a swarm of particles that work together to find the best position that corresponds with the best problem solution and according to the original position to a new one.

The fitness function will be formulated using different approaches. One utilizes a calculation model based on the domain problem to build this function. This will help us with our work. The second approach is to assign

weights based on fuzzy logic rules. These approaches emphasize the importance of designing effective fitness in PSO to get high-quality solutions. The fitness function is related to the objective function. To minimize or maximize this function, one can use PSO, so we will be focused on maximizing the objective function in order to improve the results:

$$\text{Max. } f(x_1, x_2) = 21.5 + x_1 \sin(4\pi x_1) + x_2 \sin(20\pi x_2) \quad (4)$$

$$\text{Where } -3.0 \leq x_1 \leq 12.1 \quad \text{and} \quad 4.1 \leq x_2 \leq 5.8$$

This research evaluates the ground state binding energy of odd-mass isotopes using three models: accuracy, correlation coefficient R, and mean square error. Next, an artificial neural network (ANN) is estimated. An ANN combines two inputs and two hidden layers to produce a single input. Furthermore, the PSO algorithm's optimization function verifies the accuracy and correctness of the work. Thus, it will be used to improve the number of hidden layers and learning rate of the ANN and decrease ANN error by comparing the results with the output values, mean square error of the target values, and results estimated by the ANN.

Binding Energy (BE):

In nuclear physics, the binding energy of a nucleus is the amount of energy needed to separate each of its constituent nucleons (protons and neutrons) completely (Нікіфоров and Скоренький, 2012). Analyzing binding energy requires applying a variety of nuclear models to represent proton and neutron interactions where nuclei's behavior, stability, and the energy needed to hold its constituents together are all explained by these models. Empirical formula and two theoretical models were utilized in this study: binding energy equation from the experiment, which uses the mass difference as $B.E = \Delta mc^2$. The second approach, known as the liquid drop model or the Weizsaecker semi-empirical mass formula (SEMF), views the nucleus as an incompressible nuclear matter droplet. A nucleus's total binding energy is calculated using a formula which accounts for different contributions (Aldawdy and Al-jomaily, 2022):

$$B = a_v A - a_s A^{2/3} - a_c \frac{Z(Z-1)}{A^{1/3}} - a_{sym} \frac{(N-Z)^2}{A} + \delta(A, Z) \quad (5)$$

where empirical coefficients (a_v, a_s, a_c, a_{sym} , and pairing coefficients) are obtained by fitting the model to experimental data. An extensive theoretical framework for characterizing the properties of atomic nuclei is the Integrated Nuclear Model (INM) (Ghahramany, Gharaati and Ghanaatian, 2012), where a new formula for binding energy of all nuclides will introduced based upon

intuitive assumptions. The INM is an attempt to include a wide range of nuclear properties and behaviors using his unifying approach (Ghahramany, Gharaati and Ghanaatian, 2012):

$$B(Z, N) = \left\{ \left[A - \left(\frac{(N^2 - Z^2) + \delta(N - Z)}{3Z} + 3 \right) \right] \frac{m_N c^2}{\alpha} \right\},$$

$A > 5$ (6)

Results and Discussion:

For odd mass number $17 \leq A \leq 339$ nuclei, of which there were 3414 nuclei, the binding energy was determined by combining experimental data as well as the models (LDM and INM). After that, the nuclear binding energy was computed using an Artificial Neural Network (ANN) and compared to the results of the empirical, LDM, and INM models. ANN was used to estimate the mean root square error, and the PSO algorithm was used to optimize the outcome.

The role of optimization PSO determines which Artificial Neural Network (ANN) parameters are optimal for each model in order to determine the optimal mean error square (MES), as shown in Table 1.

The results of the ANN were enhanced by a random optimization algorithm, as illustrated in each of the figures below, and the mean square error (MSE) and correlation of the input binding energy calculated by the (exp., LDM, and INM) with the results of the output by the ANN. Additionally, the error ratio and accuracy of the calculations were determined. Finding the weight value of each link in a neural network that will cause the output to most closely resemble the actual target values is the goal of the training process for an artificial neural network (ANN).

Table 1. The best parameters of the ANN for each model selected by ANN-PSO to choose the best MES:

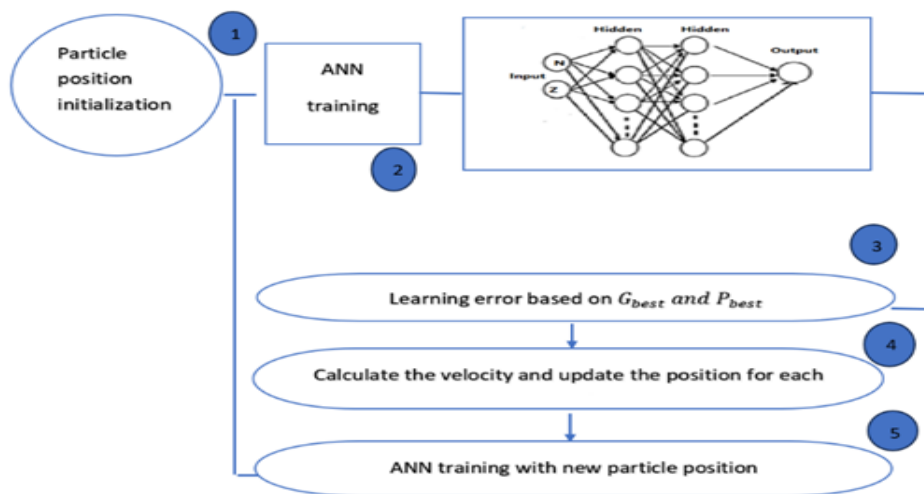
ANN Paramet.	Exp. Mode 1	LDM Mode 1	INM Mode 1	By PSO We get →	PSO ANN Paramet.	Exp. Model	LDM Model	INM Model
Learning Rate	0.5				Learning Rate	0.6341	0.1324	0.7091
N. of Neurons in Hidden L1	10				N. of Neurons in Hidden L1	22	1	10
N. of Neurons in Hidden L2	10				N. of Neurons in Hidden L2	18	1	26

Every particle is initially put into the search space at the beginning of the process. Three factors influence the particle movements for every iteration:

1. The current velocity.
2. The best performance.
3. The best performance in its neighborhoods.

Figure 3 depicts the general idea behind PSO operation.

Figure 3. The Structure of ANN-PSO Models utilized in this study.



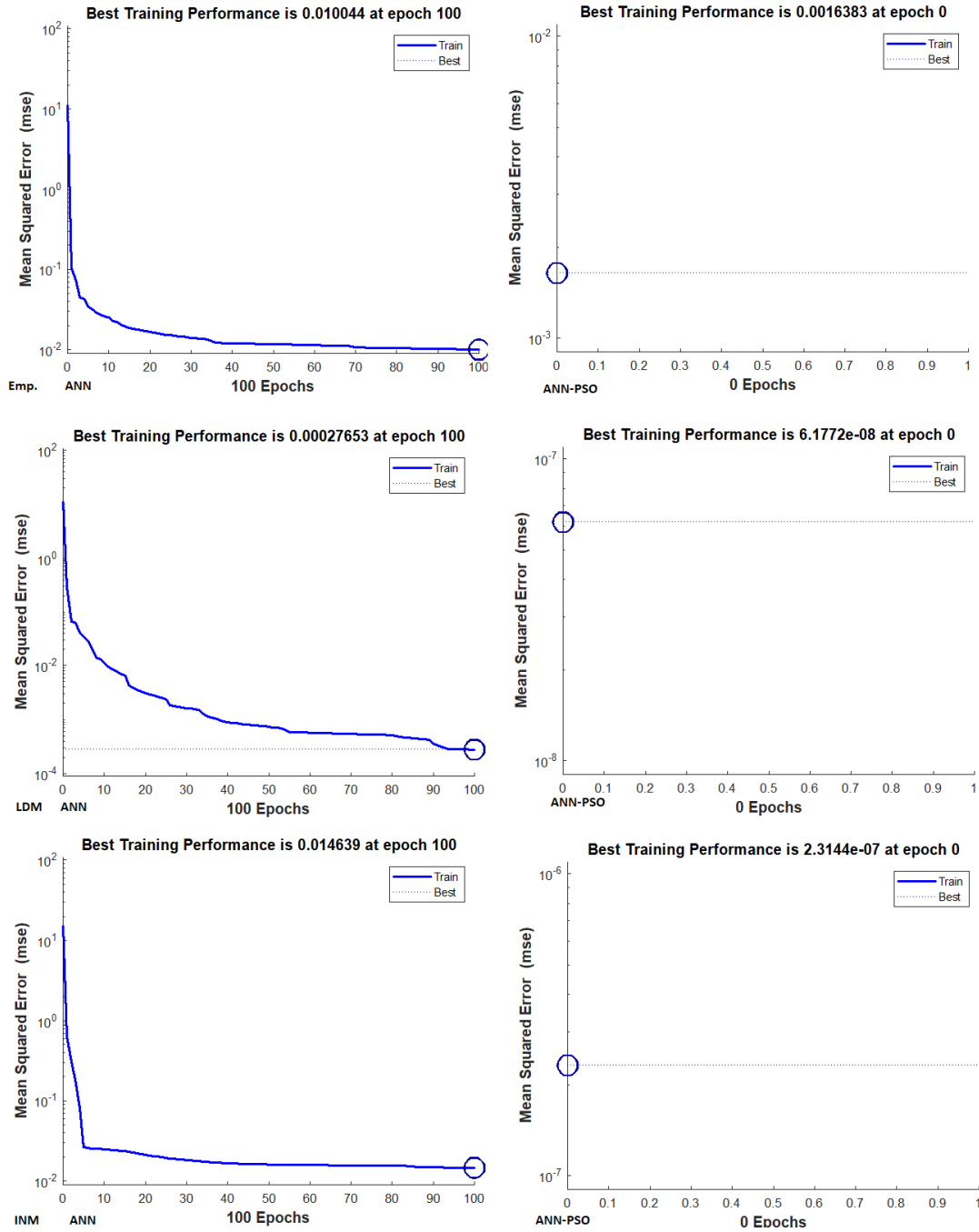


Figure 4. Best Training Performance of Mean Square Error (MSE) by ANN and ANN-PSO.

The performance of the ANN in calculating the mean square error (MSE) for the three models is shown in Figure 4. For the empirical formula, the MSE started at 101 and gradually decreased until it reached the best training performance at 0.010044 at 100 epochs in the ANN. When ANN-

PSO optimized the MSE, it settled at the best training, which was 0.0016383 at 0 epochs (The results were optimized, and 0 epochs were selected, i.e., we rounded it up because the values are small and close to 0 at ANN-PSO at the beginning of the Best MSE tends to penalize larger errors more heavily, which aligns with our objective to minimize significant deviations in the model's predictions. This makes ME a more appropriate choice for the types of predictions and error distributions we are dealing with in this study). In contrast, for the LDM model, the MSE was at ANN starting from the value 101 and gradually training at the value 0.00027653 in 100 epochs. When the MSE was optimized by PSO, it settled at the value of 6.1772×10^{-8} at 0 epochs. The INM model's value began at 12 and decreased progressively until it stabilized at 0.014639 after 100 epochs. Similarly, the PSO's MSE stabilization occurred at 2.3144×10^{-7} at 0 epochs after optimization. In Figure 5, which depicts regression and illustrates the degree of correlation between the binding energy computed by the three models and the ANN results, the target input data for the model is represented by the x-axis, and the y-axis represents the output. From the left, we can see how widely distributed the samples are on the zero line (Fit) for each model, and the value R, which indicates the mean value where it was in the experiment, was equal to $R=0.9824$. However, after using the PSO function to optimize the result, the value changed to $R=0.99715$, which indicates how much the spread of samples on the zero-line fit has improved the value of R. Regarding the second model, LDM, the value of R before ANN optimization was equal to $R=0.99955$ and after PSO it was equal to $R=1$. Similarly, the third model, INM, which ANN calculated, was equal to $R=0.99001$, and after ANN-PSO it was equal to $R=1$.

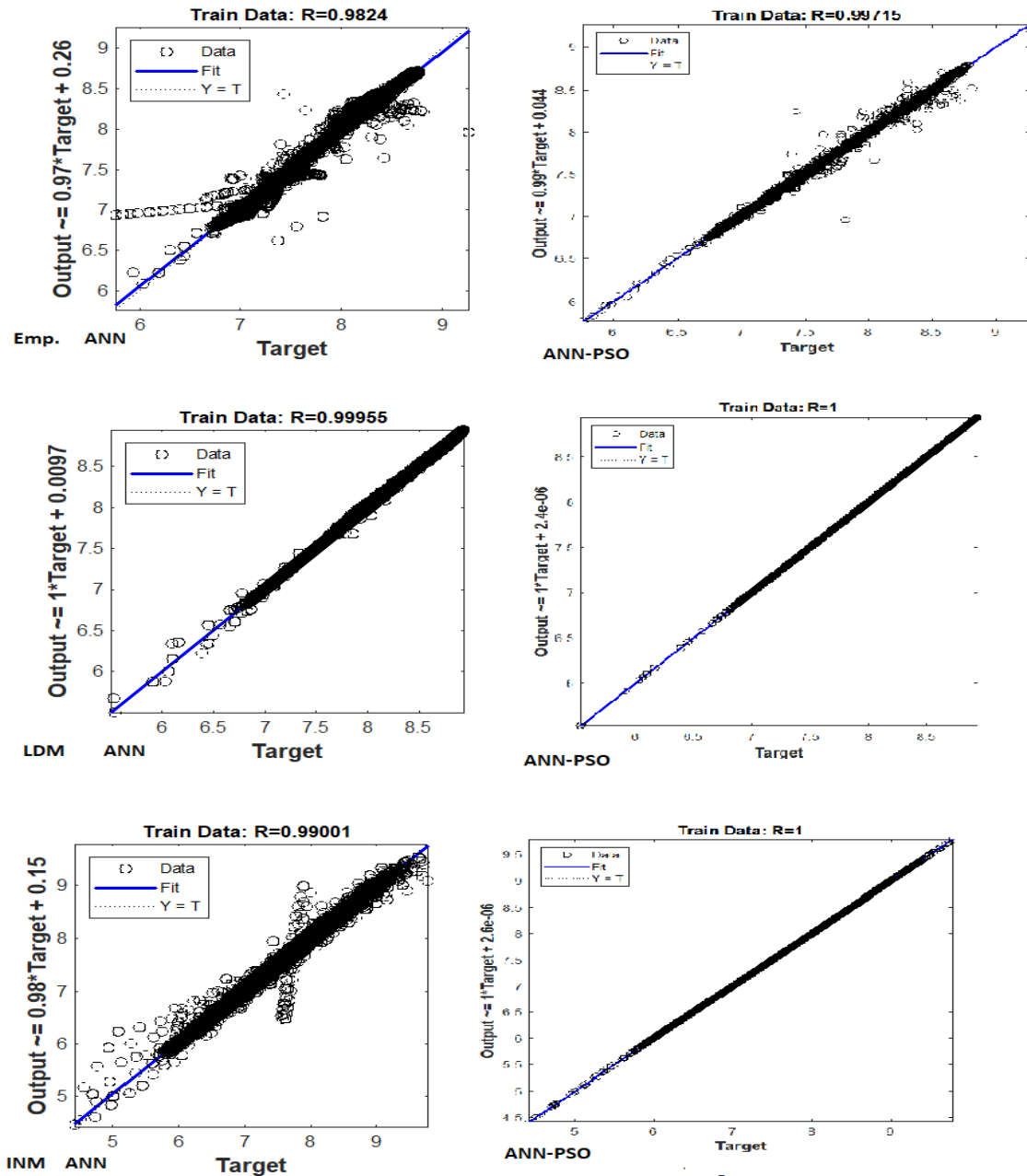


Figure 5. The regression for correlation between the value of binding energy of (Exp., LDM, and INM) with the binding energy of ANN.

Figure 6 displays an error histogram between the error value on the x-axis, which was calculated based on the difference between the output of the binding energy calculated by ANN and the result of the binding energy calculated according to the three models. The y-axis indicates the instances of

the results, where 3414 samples were collected in 20 pins, i.e., formed in the form of totals. In the first case, as per the model exp., prior to the optimization by ANN-PSO, the most severe error value was 0.000991 at Instance 2750, followed by 250 columns at the values -0.122 and 0.124. For the ANN-PSO optimization, the error closest to zero and the most severe was equal to -0.02301 at Instance 2850, then the column at Intensity 450 with the error value of 0.06107. After optimization by ANN-PSO, the error value of the model LDM became the highest instance 2750 in the column whose error value is equal to -33×10^{-5} and followed by the column with error 0.000307 at Instance 400, whereas, before optimization, the error value was at the most severe column closest to the zero-value equal to 0.001998 at Instance 2400, roughly followed by the column whose error value is equal to -0.001877 at Instance 500. Regarding the error in INM, prior to optimization, its value was -0.04819 at Instance 1700, followed by a column with an error value of 0.06628 at Instance 1300. Following PSO optimization, we observe that the error is getting closer to zero, and the outcome improved to 6.29×10^{-5} at Instance 1400, after which comes the column with an error value of 0.00043 at Instance 600.

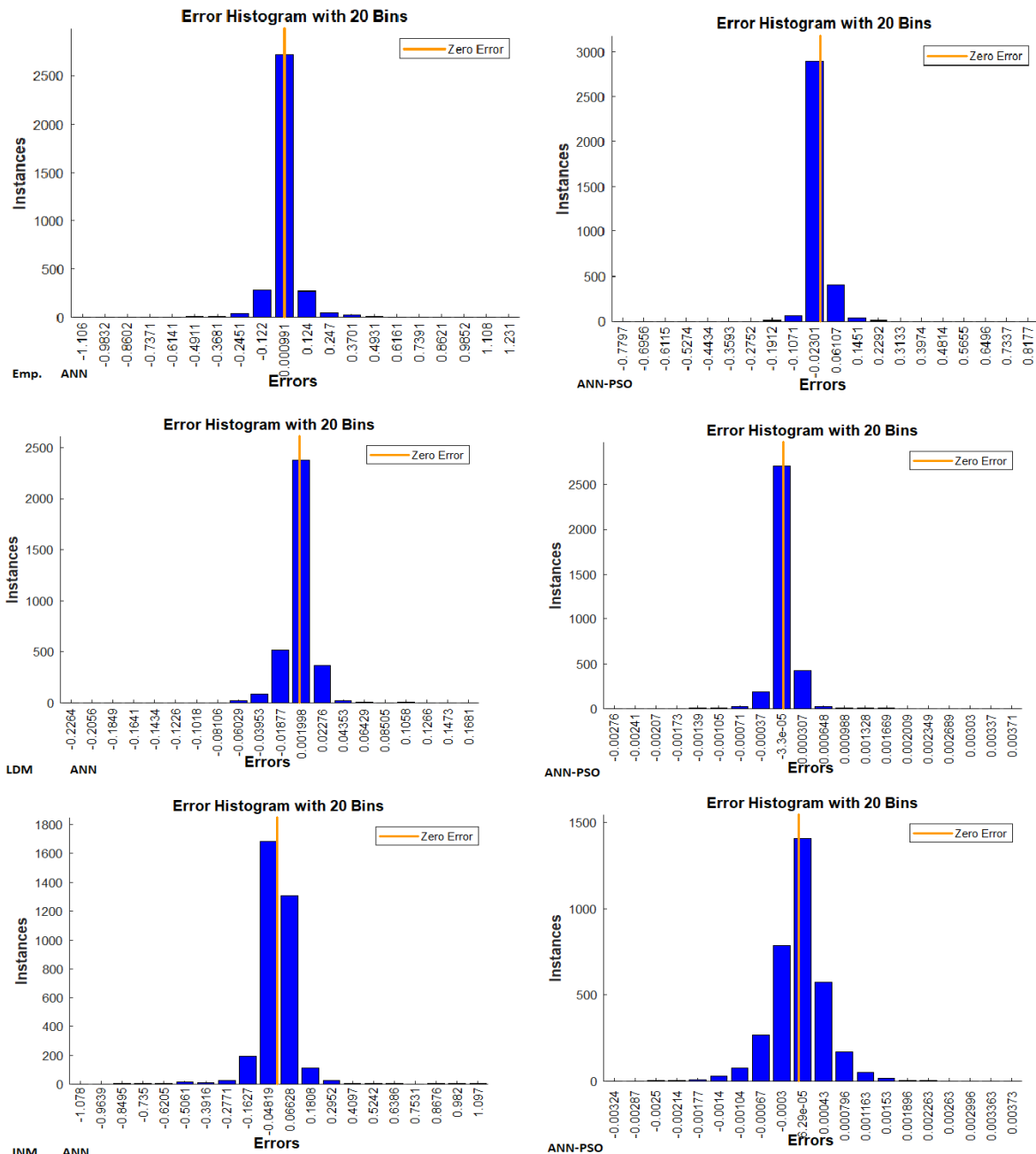


Figure 6. Error histogram in 20 pins for values of binding energy by ANN and optimized by PSO in Exp., LDM, and INM models.

In order to assess the training efficacy of every measurement tool utilized and compare the error resulting from applying each tool to the training data that was included in it, Figure 7 illustrates an error in the cumulative distribution function (CDF) for every model. This error suggests that our predictions may be within a specific range of accuracy. For the training error in the experimental case, the error value started at the value (-

1.1677) with a straight line and gradually climbed from (-0.45476) with a sloping line until it stabilized at the error value (0.36961) and the accuracy of 99.385%, as shown by the CDF for the three models. The error value exhibited a considerable decrease both prior to and following the PSO optimization. It began at -0.8217 and steadily increased until it reached the error value of 0.15953, with an accuracy of 99.443%. Regarding the LDM, we observe that the training error via (CDF) had a straight line beginning at an error value (-0.23679) and then a gradual sloping line ascending from the value (-0.0567) until it stabilized at the (0.97097) with the highest accuracy of 99.736%.

Following ANN-PSO optimization, the error scheme started to gradually ascend from the value (-0.0029254) until it stabilized at the error value (0.0010556) with the highest accuracy of 99.443%. The scheme CDF started at an error value (-1.1356) with a straight line and gradually ascended with a sloping line from the value (-0.56995) until it stabilized at training error (0.43014) at the highest accuracy of 99.385%. We also observed that the error scheme, after optimization by ANN-PSO, started to gradually ascend from the value (-0.0034206) until it stabilized at the training error value (0.001373) with an accuracy of 99.209%. The results were nearly identical to INM in terms of accuracy.

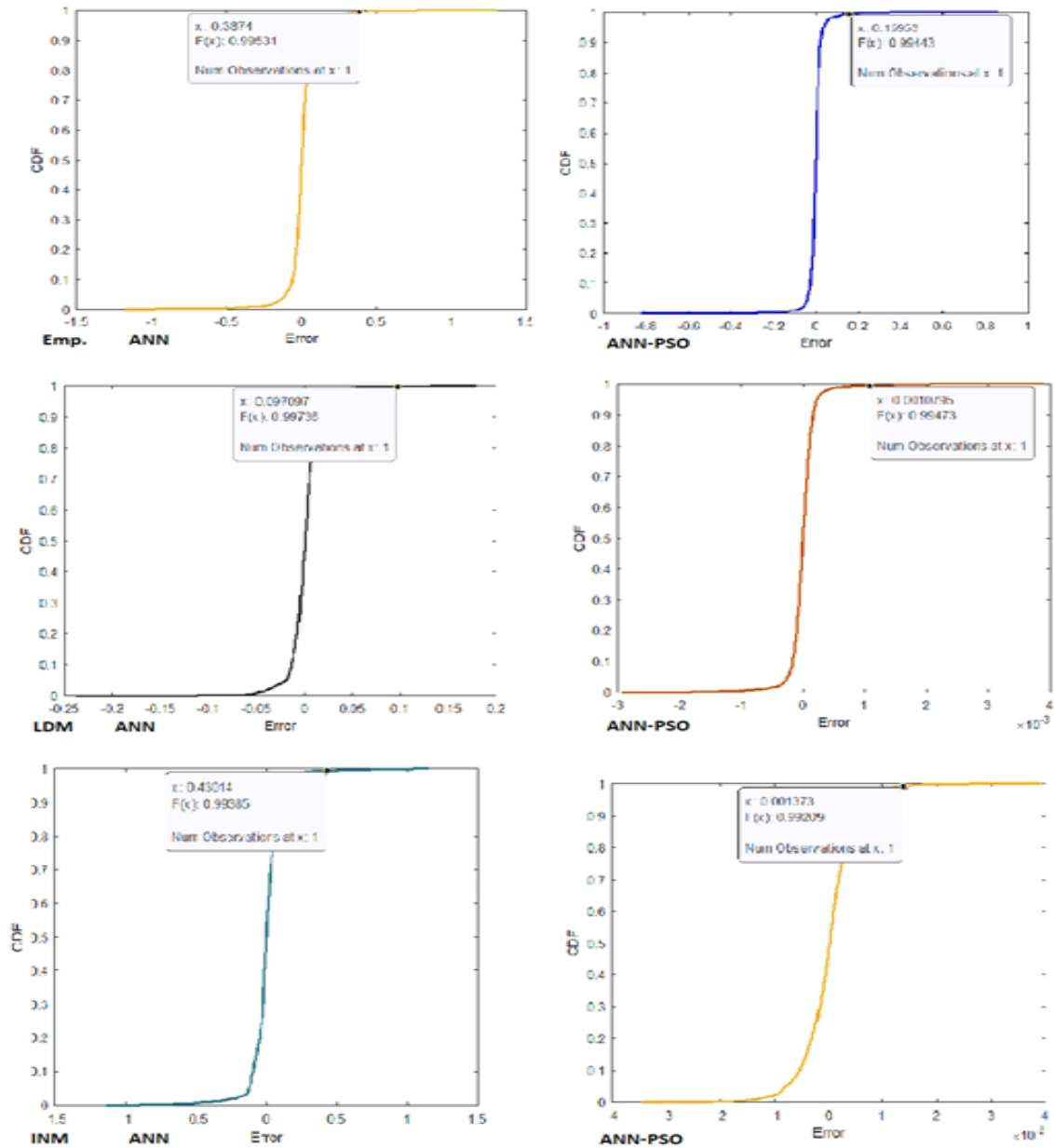


Figure 7. The CDF error scheme on the training data and the accuracy of results for ANN and ANN-PSO.

While accuracy explores the average mistake, precision looks into the distribution of error. A localization strategy that shows an error distribution with more minor errors happening more frequently than more significant errors is the recommended approach. So, when examining the accuracy of the localization techniques using the cumulative distribution function (or CDF) of error distance (Liu *et al.*, 2007). The best model for calculating binding energy is obtained through the use of ANN, and after the optimization by PSO, the three models were compared and the LDM model is better than the other two models because it obtained the highest accuracy among the three models (see Fig. 8 for 100 epoch locations with best training performance, CDF plot of the mean sequer error obtained using the constructed ANN and three models is 0.0099706).

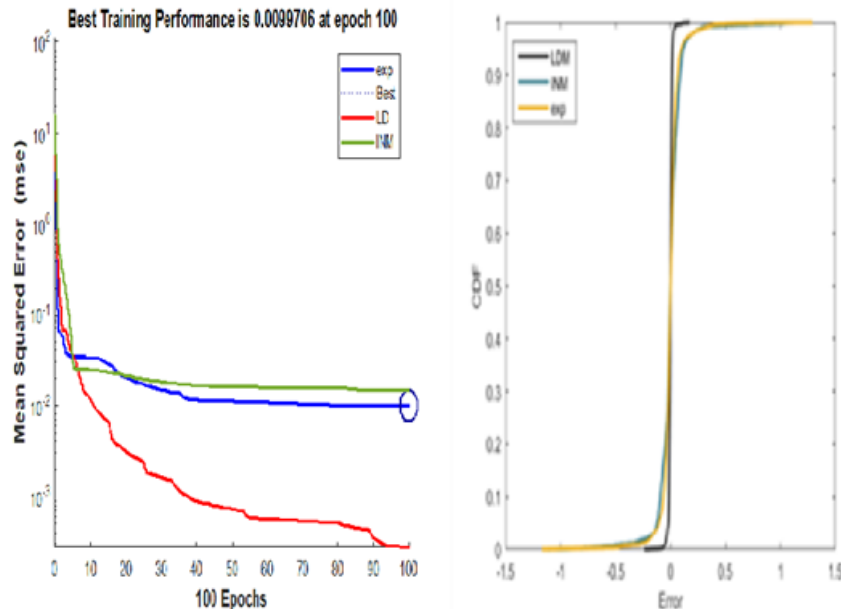
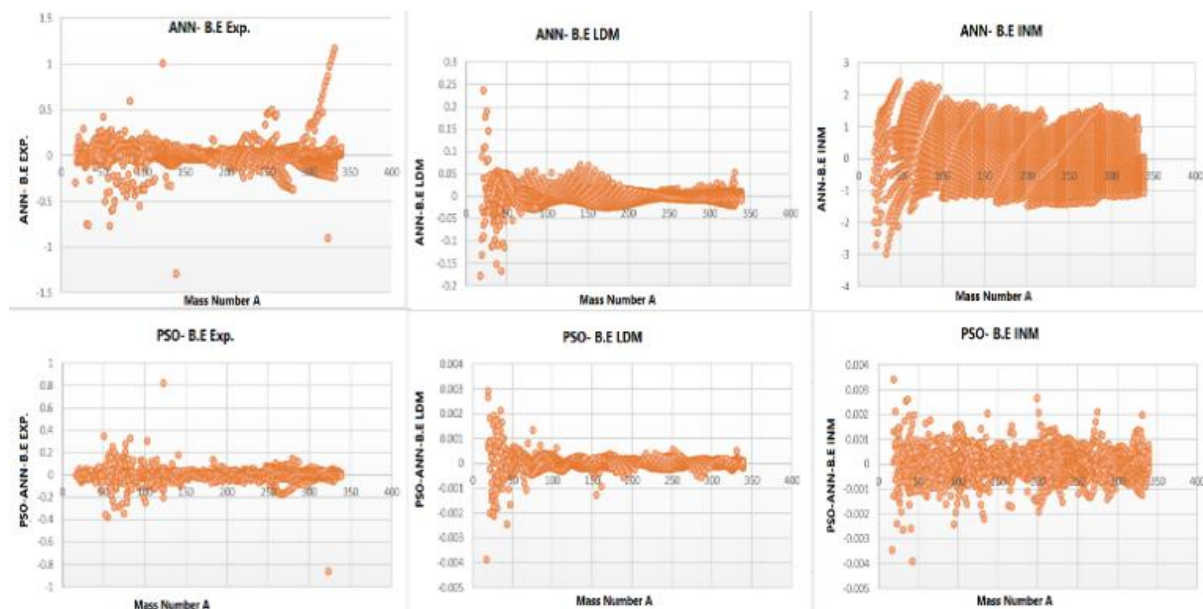


Figure 8. Show the best training and the cumulative distribution function-CDF error scheme for the result in ANN for Expt. and LDM, INM Models.

The accuracy of the data and its distribution near the zero line was calculated by calculating the difference between the results by ANN and the computational results of the three models, as well as calculating the difference between the results improved by the optimization function of the PSO and the computational results of the three models. This was done through the computational results obtained for the nuclei and their isotopes according to the (ext., LDM and INM) models, the theoretical results of the binding energy calculated by the artificial neural network, and the results improved by the PSO, and the observations of the extent of distribution and accuracy of the data in the model for LDM and its proximity to zero before



and after optimization and reduction the INM model's minimal error rate that can be adhered to, as seen in Figure 9.

Figure 9. The difference between the binding energy in three models with ANN and PSO results.

Conclusion:

The different simulations utilized in this work demonstrated that the neural network's computational structures can accurately represent a wide range of experimental and theoretical data regarding nuclear binding energy. Additionally, the neural network demonstrated exceptional efficacy in predicting and extrapolating the results within the framework of this work, which begins with the most basic options for algorithmic, coding, and training implementation. It is evident from our work that the nuclear binding energy results for the investigated odd mass number nuclei were well predicted.

In light of these facts, this study suggests including even mass nuclei for a more comprehensive understanding. Furthermore, exploring the potential of the proposed models in different datasets or nuclear properties to assess the generalization ability. Finally, this study suggests utilizing different optimization techniques to enhance the results further and offer in-depth insight into nuclear structure.

References

1. Akkoyun, S., Bayram, T. and Turker, T. (2014) 'Estimations of beta-decay energies through the nuclidic chart by using neural network', *radiation Physics and Chemistry*, 96, pp. 186–189.
2. Aldawdy, F. and Al-jomaily, F.M.A. (2022) 'Fitting the Nuclear Binding Energy Coefficients for Liquid Drop Model and Adding a mathematical terms to the Closed Shell of Magic Nuclei', *Arab Journal of Nuclear Sciences and Applications*, 55(4), pp. 150–160.
3. Audi, G. *et al.* (2017) 'The NUBASE2016 evaluation of nuclear properties', *Chin. Phys. C*, 41(3), p. 30001.
4. Audi, G., Wapstra, A.H. and Thibault, C. (2003) 'The Ame2003 atomic mass evaluation:(II). Tables, graphs and references', *Nuclear physics A*, 729(1), pp. 337–676.
5. Bahdanau, D. (2014) 'Neural machine translation by jointly learning to align and translate', *arXiv preprint arXiv:1409.0473* [Preprint].
6. Bishop, C. (2006) 'Pattern recognition and machine learning', *Springer google schola*, 2, pp. 531–537.
7. Chan, W. *et al.* (2016) 'Listen, attend and spell: A neural network for large vocabulary conversational speech recognition', in *2016 IEEE international conference on acoustics, speech and signal processing (ICASSP)*. IEEE, pp. 4960–4964.
8. Chen, L.-C. *et al.* (2018) 'Searching for efficient multi-scale architectures for dense image prediction', *Advances in neural information processing systems*, 31.
9. Costiris, N.J. *et al.* (2009) 'Decoding β -decay systematics: A global statistical model for β -half-lives', *Physical Review C—Nuclear Physics*, 80(4), p. 44332.
10. Duflo, J. and Zuker, A.P. (1995) 'Microscopic mass formulas', *Physical Review C*, 52(1), p. R23.
11. Feurer, M. and Hutter, F. (2019) 'Hyperparameter optimization', *Automated machine learning: Methods, systems, challenges*, pp. 3–33.
11. Fu, G.J. *et al.* (2011) 'Description and evaluation of nuclear masses based

- on residual proton-neutron interactions', *Physical Review C—Nuclear Physics*, 84(3), p. 34311.
12. Garvey, G.T. and Kelson, I. (1966) 'New nuclidic mass relationship', *Physical Review Letters*, 16(5), p. 197.
13. Ghahramany, N., Gharaati, S. and Ghanaatian, M. (2012) 'New approach to nuclear binding energy in integrated nuclear model', *Journal of Theoretical and Applied Physics*, 6, pp. 1–5.
14. Ghiasi, G., Lin, T.-Y. and Le, Q. V (2019) 'Nas-fpn: Learning scalable feature pyramid architecture for object detection', in *Proceedings of the IEEE/CVF conference on computer vision and pattern recognition*, pp. 7036–7045.
15. Hannun, A. (2014) 'Deep Speech: Scaling up end-to-end speech recognition', *arXiv preprint arXiv:1412.5567* [Preprint].
16. Hassoun, M.H. (1995) *Fundamentals of artificial neural networks*. MIT press.
17. He, K. *et al.* (2016) 'Deep residual learning for image recognition', in *Proceedings of the IEEE conference on computer vision and pattern recognition*, pp. 770–778.
18. Hutter, F., Kotthoff, L. and Vanschoren, J. (2019) *Automated machine learning: methods, systems, challenges*. Springer Nature.
19. Jiang, H. *et al.* (2010) 'Nuclear mass relations based on systematics of proton-neutron interactions', *Physical Review C—Nuclear Physics*, 82(5), p. 54317.
20. Jiang, H. *et al.* (2012) 'Predictions of unknown masses and their applications', *Physical Review C—Nuclear Physics*, 85(5), p. 54303.
21. Jiao, B.B. (2020a) 'Nuclear binding energy predictions based on BP neural network', *International Journal of Modern Physics E*, 29(05), p. 2050024.
22. Jiao, B.B. (2020b) 'The study of Nuclear binding energy for $A \geq 100$ based on Odd-Even staggering of nuclear masses', *arXiv preprint arXiv:2005.04636* [Preprint].
23. Kennedy, J. and Eberhart, R. (1995) 'Particle swarm optimization', in *Proceedings of ICNN'95-international conference on neural networks*. ieee, pp. 1942–1948.
24. Kennedy, J. and Eberhart, R.C. (1997) 'A discrete binary version of the particle swarm algorithm', in *1997 IEEE International conference on systems, man, and cybernetics. Computational cybernetics and simulation*. IEEE, pp. 4104–4108.

25. Kondev, F.G. and Naimi, S. (2017) ‘The AME2016 atomic mass evaluation (II). Tables, graphs and references’, *Chinese Physics C*, 41(3), p. 30003.
26. Li, Z. *et al.* (2022) ‘Comparative study of meta-heuristic algorithms for reactor fuel reloading optimization based on the developed BP-ANN calculation method’, *Annals of Nuclear Energy*, 165, p. 108685.
27. Liu, H. *et al.* (2007) ‘Survey of wireless indoor positioning techniques and systems’, *IEEE Transactions on Systems, Man, and Cybernetics, Part C (Applications and Reviews)*, 37(6), pp. 1067–1080.
28. Mumpower, M.R. *et al.* (2016) ‘The impact of individual nuclear properties on r-process nucleosynthesis’, *Progress in Particle and Nuclear Physics*, 86, pp. 86–126.
29. Phommixay, S., Doumbia, M.L. and Lupien St-Pierre, D. (2020) ‘Review on the cost optimization of microgrids via particle swarm optimization’, *International Journal of Energy and Environmental Engineering*, 11(1), pp. 73–89.
30. Real, E. *et al.* (2019) ‘Regularized evolution for image classifier architecture search’, in *Proceedings of the aaai conference on artificial intelligence*, pp. 4780–4789.
31. Roca-Maza, X. and Piekarewicz, J. (2008) ‘Impact of the symmetry energy on the outer crust of nonaccreting neutron stars’, *Physical Review C—Nuclear Physics*, 78(2), p. 25807.
32. Shen, J., Khodak, M. and Talwalkar, A. (2022) ‘Efficient architecture search for diverse tasks’, *Advances in Neural Information Processing Systems*, 35, pp. 16151–16164.
33. Szegedy, C. *et al.* (2017) ‘Inception-v4, inception-resnet and the impact of residual connections on learning’, in *Proceedings of the AAAI conference on artificial intelligence*.
34. Takamoto, S. *et al.* (2022) ‘Towards universal neural network potential for material discovery applicable to arbitrary combination of 45 elements’, *Nature Communications*, 13(1), p. 2991.
35. Thoennessen, M. (2018) ‘2017 update of the discoveries of nuclides’, *International Journal of Modern Physics E*, 27(02), p. 1830002.
36. Utama, R. and Piekarewicz, J. (2017) ‘Refining mass formulas for astrophysical applications: A Bayesian neural network approach’, *Physical Review C*, 96(4), p. 44308.
37. Utama, R. and Piekarewicz, J. (2018) ‘Validating neural-network refinements of nuclear mass models’, *Physical Review C*, 97(1), p. 14306.

38. Utama, R., Piekarewicz, J. and Prosper, H.B. (2016) ‘Nuclear mass predictions for the crustal composition of neutron stars: A Bayesian neural network approach’, *Physical Review C*, 93(1), p. 14311.
39. Vaswani, A. (2017) ‘Attention is all you need’, *Advances in Neural Information Processing Systems* [Preprint].
40. Wang, M. *et al.* (2012) ‘The Ame2012 atomic mass evaluation’, *Chinese physics C*, 36(12), p. 1603.
41. Zeng, L.-X. *et al.* (2024) ‘Nuclear binding energies in artificial neural networks’, *Physical Review C*, 109(3), p. 34318.
42. Нікіфоров, Ю.М. and Скоренький, Ю.Л. (2012) ‘Fundamentals of Nuclear Physics’, in.

سرب الجسيمات لتحسين المعلمات الفائقة ومعلمات الشبكة العصبية الاصطناعية للتنبؤ بطاقة الربط النووي لبعض نظائر الكتلة الفردية

رؤيا حروش ابراهيم⁽¹⁾ اكرم محمد علي⁽²⁾
 قسم الفيزياء، كلية العلوم، جامعة الأنبار، قسم الفيزياء، كلية العلوم، جامعة
 الرمادي، العراق الأنبار، الرمادي، العراق
dr.akram@uoanbar.edu.iq Roy21s2010@uoanbar.edu.iq

مستخلص البحث:

الشبكات العصبية الاصطناعية (ANNs) هي نماذج أساسية للتعليم الآلي تُستخدم على نطاق واسع في مختلف المجالات والتطبيقات. تعتمد هذه النماذج على متجه من المعلمات التي يجب تقديرها حسابياً. في هذه الدراسة، تم تطوير شبكة عصبونية اصطناعية متعددة الطبقات متصلة بالكامل، وهي شبكة عصبية حديثة متعددة الطبقات ذات طبقتين للمدخلات وطبقتين مخفيتين (تحتوي كل منها على 10 خلايا عصبية)، لتقدير طاقة الارتباط في الحالة الأرضية للنظائر ذات الأعداد الكتلية الفردية التي تتراوح بين 17 و339، وتغطي 3414 نواة. وطُبقت الشبكة العصبية الاصطناعية على ثلاثة نماذج: النموذج النووي المتكامل، ونموذج القطرة السائلة، والصيغة التجريبية. وتم تقييم طاقات الارتباط المتوقعة للحالة الأرضية باستخدام متوسط الخطأ المربع (MSE) ومعامل الارتباط (R) والدقة. ولتحسين أداء الشبكة العصبية الاصطناعية على النحو الأمثل، تم تحسين المعلمات مثل عدد الطبقات المخفية ومعدلات التعلم باستخدام خوارزمية تحسين سرب الجسيمات (PSO). وقد أدى هذا التحسين إلى تقليل خطأ الشبكة العصبية الاصطناعية وتحقيق معدل MSE قدره 0.0099706 ودقة عالية بلغت 99.736% لنموذج LDM. وأظهر معامل الارتباط R ارتباطاً قوياً بين الهدف وقيم المخرجات، مما يؤكد دقة النماذج ومتانتها. كما أدى تحسين خوارزمية PSO إلى تقليل الأخطاء وتحسين النتائج، مما يؤكد صحة الاختلافات في طاقة الارتباط بين النماذج الثلاثة والشبكة العصبية الاصطناعية. يؤكد هذا النهج فعالية الشبكات العصبية الاصطناعية في نمذجة الظواهر الفيزيائية المعقدة بدقة عالية.

الكلمات المفتاحية: الشبكة العصبية الاصطناعية، طاقة الربط، متوسط الخطأ المربعي، خطأ خوارزمية تحسين سرب الجسيمات خطأ، خوارزمية PSO.

ملاحظة: هل البحث مستل من رسالة ماجستير او اطروحة دكتوراه؟ نعم: ✓ كلا: